(This is a sample cover image for this issue. The actual cover is not yet available at this time.)

Journal of Manufacturing Processes 26 (2017) 142–154

Contents lists available at ScienceDirect

Journal of Manufacturing Processes

journal homepage: www.elsevier.com/locate/manpro

Technical Paper

Tool geometry optimization in friction stir spot welding of Al-steel joints

Joaquín M. Piccini[a,*], Hernán G. Svoboda[a,b]

[a] Welding Technology Group, Materials and Structures Laboratory, INTECIN, Facultad de Ingeniería, Universidad de Buenos Aires, Buenos Aires, Argentina
[b] National Council of Scientific and Technical Research (CONICET), Buenos Aires, Argentina

ARTICLE INFO

Article history:
Received 8 September 2016
Received in revised form 26 January 2017
Accepted 4 February 2017

Keywords:
Friction stir spot welding (FSSW)
Tool indentation
Dissimilar joints

ABSTRACT

The necessity to reduce the weight of transport structures, such as cars and airplanes, has become more important due to gas emission regulations. In this regard, the use of hybrid structures made of steel and aluminum is a way to achieve this goal. Joining aluminum to steel is a great challenge and Friction Stir Spot Welding (FSSW) has become as a new potential welding technique to produce dissimilar joints. Despite Friction Stir Welding has been studied on different similar joints, the information related to the influence of FSSW parameters on the evolution of aluminum-steel joints is scarce. So, the effect of the tool geometry and its penetration depth during FSSW of AA5052–LCS (Low Carbon Steel) joints, has been studied. During FSSW, axial load and consumed electrical current were recorded in order to improve the understanding of the welding process. Macro and microstructural characterization was done on the cross section of the welded spots. The mechanical properties of the joints were determined by microhardness profiles and by Peel and Cross Tension tests. The fracture loads increased when the tool penetration depth goes up. The tool geometry optimization also increased the fracture loads.

1. Introduction

Fuel efficiency, lowering carbon emissions and passenger safety have been the main drivers in designing automobiles for the past twenty years. In this sense, vehicle weight reduction was identified as a key strategy to minimize fuel consumption [1]. Lightweight materials such as aluminum and magnesium, when properly designed, can be used to replace equivalent steel assemblies with approximately half the weight [2]. The main use of this material on cars structures has been on closure panels such as hoods, doors and lift gates to reduce weight and improve vehicle fuel economy [2]. Current closure panel joining techniques include Resistance Spot Welding (RSW), Self-Pierce Riveting, and clinching [2]. However, the disadvantages of these methods to weld aluminum sheets include weld electrode dressing, high energy consumption, and the use of consumables that add weight to the structures. The welding method used for aluminum sheets is one of the key technology drivers to enhance weight reduction in the automotive industry, and hence, Friction Stir Spot Welding (FSSW) is being considered as an alternative joining technique [2]. The use of aluminum parts in cars structures implies the joining of aluminum and steel sheets. Joining dissimilar materials may present the advantages of both materials, offering solutions to specifics engineering problems but often presenting more difficulties. Joining of Al to steel sheets has become very important in the industry and several joining methods including fusion arc welding processes, laser beam welding, resistance welding, mechanical joining, brazing, Cold Metal Transfer, hot bonding or even hybrid joining techniques have been considered [3].

Several aspects have to be considered when a dissimilar joint is going to be designed. The main are: joint geometry, sheets thicknesses, thermal distortions, galvanic corrosion, residual stress because of welding and joint mechanical properties. Depending on the specific process, other aspects have to be also considered: melting points, formation of intermetallic compounds and the effect of the thermal cycle during welding on the microstructural evolution of the base materials [4]. The main problem when welding aluminum with steel is the metallurgical evolution of the joint related to the formation of Inter Metallic Compounds (IMC). The thermal cycle during welding may form different intermetallic compounds in the interface between both materials and during solidification

Abbreviations: FSSW, friction stir spot welding; RSW, resistance spot welding; IMC, inter metallic compounds; TPD, tool penetration depth; PT, peel test; CT, cross tension; BM, base material; HAZ, heat affected zone; TMAZ, thermo mechanical affected zone; SZ, stir zone; SEM, scanning electron microscope; LCS, low carbon steel.

* Corresponding author.
E-mail address: joaquin.piccini@gmail.com (J.M. Piccini).

http://dx.doi.org/10.1016/j.jmapro.2017.02.004
1526-6125/

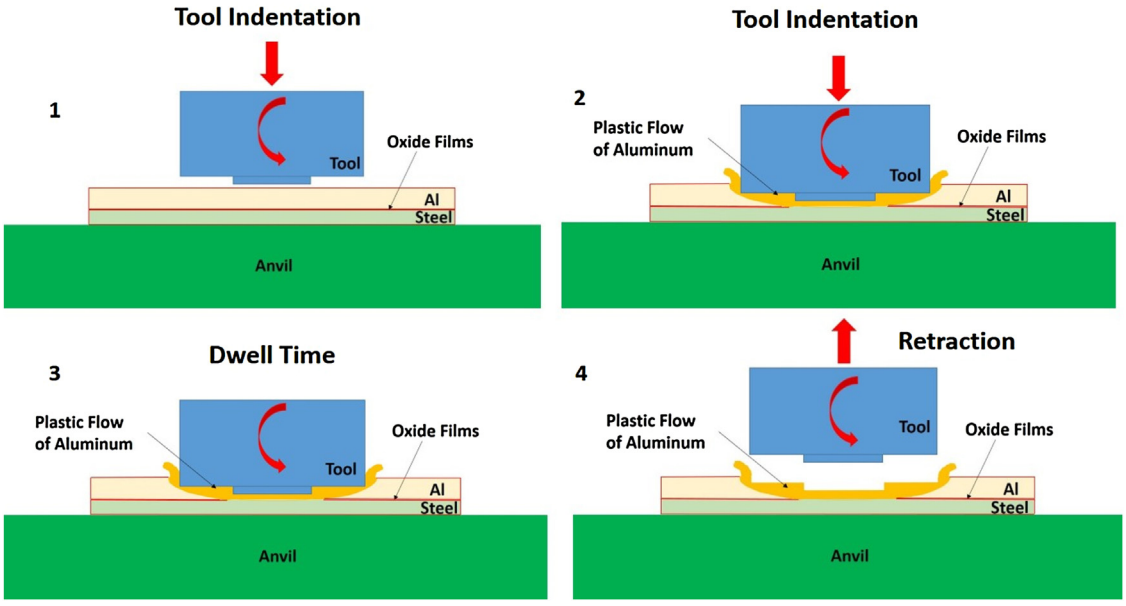

Fig. 1. Friction Stir Spot Welding of Aluminum to steel sheets.

Table 1
Chemical composition of the materials used (wt%).

Material	C	Si	Fe	Cu	Mn	Mg	Zn	S	Cr	P
AA5052-H32	–	0.06	0.25	0.01	0.01	2.38	0.005	–	0.16	–
LCS	0.08	0.10	Bal.	–	0.40	–	–	0.025	–	0.025

of the diluted zones. Formation and growth of IMC may occur during conventional fusion welding processes and even in solid state joining processes. When the heat input is increased, the thickness of the intermetallic layer that grows in the interface between the materials being joined also rises [4].

FSSW technique was invented by Mazda [2]. It is a solid state welding process which has three main steps, as it may be appreciated in Fig. 1. In first place, a rotating non consumable tool with a pin is plunged into the two sheets that are going to be welded in a lap configuration (steps 1 and 2 in Fig. 1). At the same time, a backing plate, or anvil, contacts the lower sheet from the bottom and supports the axial load made by the welding tool during the welding cycle. Also, in this first step, the geometry of the tools shoulder gives compressive force to the materials. In the third step, when the tool penetration depth is reached, the downward movement stops ant the welding tool is held in that place for a certain period of time, known as dwell time. In this step, heated and softened material due to the welding action causes plastic flow. Finally, in the fourth step, the welding tool is retracted from the sheets while a solid state joint has been made between the upper and lower sheet. This technology was first used in Mazda RX-8 aluminum rear door panel spot welding in 2003 [2].

Since the required heat input in a solid state joining process, such as FSSW, is much less than that of the RSW, nowadays FSSW has been regarded as one of the most available method for the dissimilar welding of Al to steel alloys [5].

The appropriate selection of the welding parameters of FSSW would control the microstructural evolution of the joint and may produce sound joints with low thermal cycles. Tool geometry, tool rotation speed, dwell time and tool penetration depth are considered as the main FSSW welding parameters [6–10]. Finally, another critical factor in the joint strength in aluminum/steel friction stir joining is the tool penetration depth (TPD) into the steel sheet [11,12]. According to [11,12], as much as the tool penetrates the steel sheet, lower is the thickness of the intermetallic layer and higher is the inter mix between sheets, improving welds strength. Previous works, have shown that when the tool slightly runs into the steel surface, the joint strength is greater than that when the probe tip does not reach the steel surface [6,7]. However, more complex tool materials with much higher strength than steel, such as carbides or other ceramics like Polycrystalline Cubic Boron Nitride, have to be used. Nevertheless, it is possible to use cheaper tool materials and still promote bonding via diffusion without penetrating the tool into the lower sheet [10]. In Fig. 1 the main steps of this welding process are shown.

Joining Al/St sheets is still of great interest, especially when welding thin sheets without inter mix between Al and steel, with cheap welding tools. According to [9], tool design is a key factor when welding Al/St thin sheets by FSSW. It has been appreciated that a plastic instability occurs, when welding with high levels of TPD, on the aluminum sheet, causing high deformations of it and weld defects. It has been previously reported that Al/St thin sheets may be joined using a tool made of a common H13 [13]. However, the shoulder remains relatively far from the interface and mechanical properties were not high enough [13]. It has been previously reported that the optimal TPD is 0.85 mm when welding with a tool shoulder and probe diameter of 10 and 2 mm, respectively [14]. However, for high levels of TPD a plastic instability of the aluminum sheet was also appreciated [9,14]. On the other hand, it has been observed that the optimal mechanical properties are achieved when the shoulder of the welding tool gets closer to the joint interface [15]. It is worth noticing that previous works have used long dwell times of 5 s [9,14] up to 15 s [16]. These dwell times are too high taking into account the productivity of an assembly process and its optimization is a pending matter.

The aim of this work was to design FSSW tools able to weld Al/St thin sheets without defects. Moreover, the effects of tools geometry and its penetration depth on the weldability and mechanical

Table 2
Analyzed welding conditions.

Sample	TPD (mm)	Welding Tool	Sample Type
5-A	0.05	A	P-C-M
20-A	0.20	A	P-C-M
25-A	0.25	A	P-M
35-A	0.35	A	C
55-A	0.55	A	P-C-M
5-B	0.05	B	P-M
20-B	0.20	B	P-M
25-B	0.25	B	P-M
35-B	0.35	B	P-C-M
45-B	0.45	B	P-C-M
55-B	0.55	B	P-C-M
5-C	0.05	C	P-C-M
10-C	0.1	C	P-C-M
20-C	0.2	C	P-C-M
25-C	0.25	C	M
30-C	0.3	C	P-M
40-C	0.4	C	P-C-M
50-C	0.5	C	P-M
65-C	0.65	C	P-M

properties of dissimilar AA5052-H32 with Low Carbon Steel (LCS) joints welded by FSSW, was investigated.

2. Experimental procedure

2.1. Base materials and FSSW samples

Friction Stir Spot welds were carried out on dissimilar lap joints made of AA5052-H32 and an LCS of 1 mm and 0.65 mm thick, respectively. The chemical composition of the materials used can be appreciated in Table 1. It may be seen that the AA5052-H32 is an Aluminum-Magnesium alloy, with little amounts of Fe. The H32 condition means that the sheet used, had been cold worked. The microhardness of this material was 80 HV. The LCS used has low amounts of C and Mn, as common deep drawing steel, having a microhardness of 100 HV.

The aluminum sheet was always placed on top of the lap joint. In the present paper the design of the welding tool, in order to optimize the FSSW procedure was investigated, as well as the effect of the TPD on the microstructural evolution and mechanical properties of the welded joints. Thus, three welding tools were design in order to improve the welding procedure. Every single tool was made of H13 tool steel with a concave shoulder of 11.8 mm.

Taking into account the results shown by [9,13,14], the welding tool "A" had a tapered pin with 0.3 mm in length and 5 mm in diameter at the end, in order to improve the mechanical properties of the welded spots and to avoid plastic instability of the aluminum sheet.

The "B" tool was pinless in order to weld with higher levels of TPD and higher heat inputs, improving mechanical properties of the welded spots [15].

Finally, the "C" tool had a tapered pin of 0.4 mm in length and 9.6 mm in diameter at its end. This design is proposed in order to achieve the advantages of the "A" and "B" tools (no plastic instability of the aluminum sheet, high levels of TPD and high heat input), reducing their disadvantages.

Every single welded spot was done with a penetration rate of 35 mm/min, a dwell time of 2 s and a rotational speed of 1200 RPM. Table 2 lists the analyzed welding conditions and the identification used for each sample.

It can be appreciated that the TPD was varied between 0.05 and 0.65 mm. For lower values of tool penetration depth, the welding of both materials could not be achieved. On the other hand, for higher tool penetration depths the tool would penetrates the steel sheet damaging the welding tools.

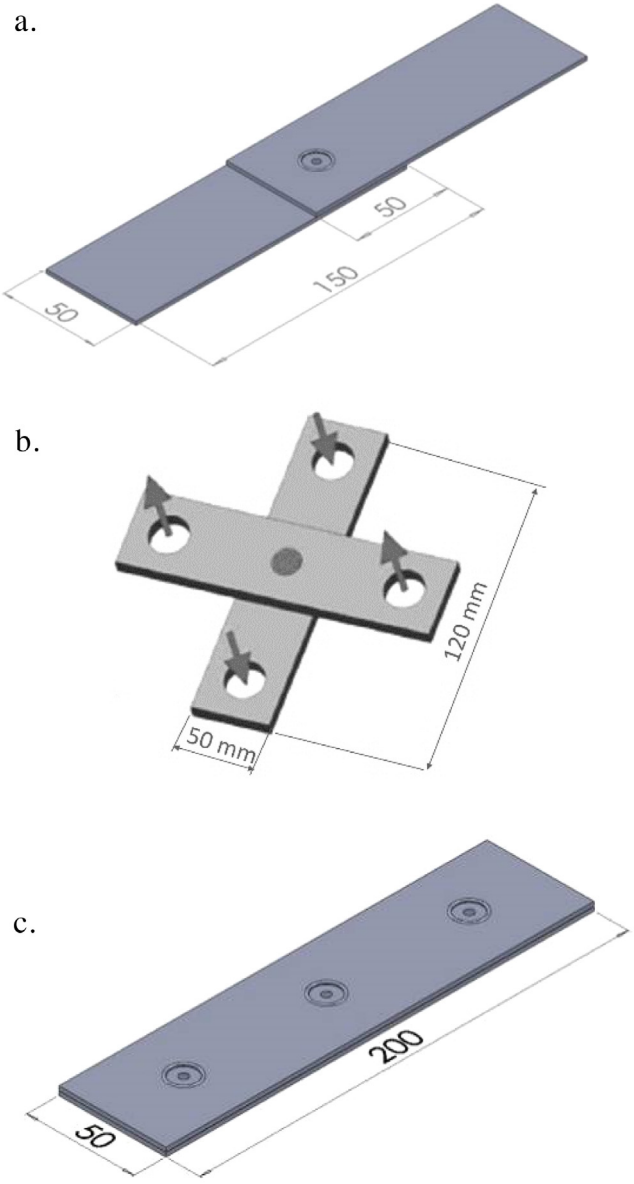

Fig. 2. Friction Stir Spot welding samples: (a) P sample, (b) C sample and (c) M sample.

In order to study the evolution of the welded joints with the tools geometry and the welding parameters, three types of joints were welded for each welding conditions. The joint called as "P" was used for Peel Test (PT), as it could be seen in Fig. 2a. The "C" sample (Fig. 2b) was welded to analyze the mechanical properties in Cross Tension Test (CT). Finally, in order to make microhardness profiles, dimensional analysis, macro and microstructural characterization, the "M" sample was welded (Fig. 2c). The types of samples produced are also indicated at Table 2. The clamping system used for FSSW of dissimilar joint could be seen in Fig. 3.

2.2. Data acquisition

In order to achieve a better understanding of the FSSW process and the evolution of the welded spots with the main welding parameters, axial load and current consumed by the machine during welding were recorded. This procedure was done using a data acquisition NI1008 system with an acquisition rate of 20 Hz. The software used was the LabView Signal Express 3.0.

Fig. 3. Friction Stir Spot welding system and clamping device.

2.3. Metallographic characterization

The samples for metallographic examination were cross sectioned and mounted as it is shown in Fig. 4a and b. After polishing, the specimens were etched with the Kellerís reagent to reveal their macrostructures.

The characteristics dimensions of the welded joints are shown in Fig. 5. It is worth noting that the TPD is defined as the shoulders penetration into the aluminum sheet, despite the geometry and shape of the pin, for all the welding tools used [2]. The distance between the surface left by the pin and the free surface of the bottom sheet is called P. Finally, the distance between the lower point of the surface left by the shoulder and the joint interface is IH, as it may be seen in Fig. 5. All the characteristic dimensions were measured on each sample by means of a stereoscopic light microscope and an image analysis software. Macrographic observations were done using light microscopy. The interface structure of the weld was analyzed by Scanning Electron Microscope (SEM).

2.4. Mechanical properties

Mechanical properties of the welds were analyzed by microhardness tests, CT and PT. Microhardness profiles were done 200 μm above the interface on the aluminum sheet with a load of 300 g and a dwell time of 10 s, according to ASTM E384. Peel and Cross Tension Tests were performed in an Interactive Instruments 1000 K machine at a constant cross-head speed of 1 mm/min. For every single welding condition, three samples were tested for each test type, in order to achieve the standard deviation of the process. Load and displacement signals were recorded, obtaining the load-displacement curves. Fracture load and fracture modes were analyzed. Light microscopy was used to observe fracture surfaces.

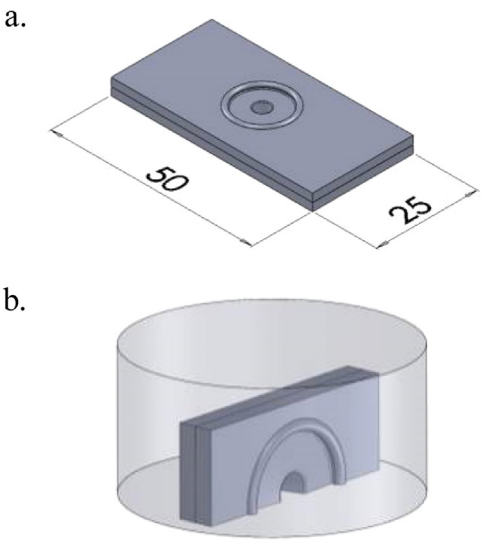

Fig. 4. M sample for metallographic analysis.

3. Results

3.1. Macrostructural characterization

The appearance of several FSS welds, done with different welding conditions, may be seen in Fig. 6a–f. It is shown that with only a dwell time of 2 s, FSSW joints were achieved with no significant defects, for all the welding conditions studied. As it has been previously reported, TPD affects heat generation and material plastic flow. So, material of the top sheet is squeezed out during the downward movement of the welding tool. Samples 5-A–5-C were welded with the lowest TPD (Fig. 6a, d and g), meanwhile samples 55-A, 55-B and 65-C were welded with the highest TPD values. The material which flows out of the spot increases with the TPD.

When the TPD reaches a maximum value, the top sheet is deformed, as it can be seen in Fig. 7.

Macrographic observations along the cross sections located at the major diameter of the spot welds, are shown in Fig. 8a–c for the different welding conditions.

Tool penetration depth produces a radial expansion of the top sheet outside the tools circumference. However, due to the imposed axial load by the welding tool, the top sheet cannot flow freely and it bends outside the contour of the welding tool. This effect goes up with the tool penetration depth (Fig. 7). It is worth noting that the welding tool never reaches the steel sheets.

It has been demonstrated that metallurgical bonds in FSSW of Al-St joints are formed as a result of the atomic diffusion across the joint interface [13]. Al/Fe IMC will be formed as a consequence of the atomic diffusion if enough energy is provided at the joint interface [16].

The geometry of the welding tools was proposed in order to improve the mechanical properties of the welding joint. According to [2] the largest part of the total heat input during FSSW is generated in the contact zone between the top plate and the shoulder of the welding tool. Therefore, a better metallurgical bonding could be achieved as much as the shoulder gets close to the interface, because higher will be its action on it. This would also require less time to produce a sound joint.

In Table 3 the measured characteristics dimensions of the joints are shown. It could be appreciated that, according to the main dimension, there is no big differences when welding with the “A” and “C” tool. On the other hand, welding with the “B” tool allows to achieve lower IH values.

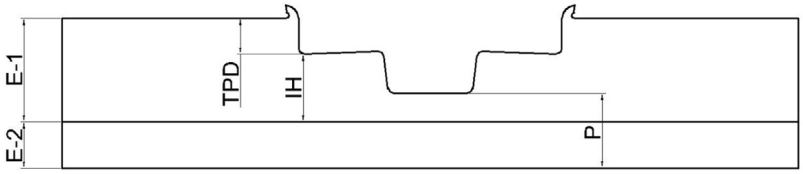

Fig. 5. Main dimensions of the welded spots.

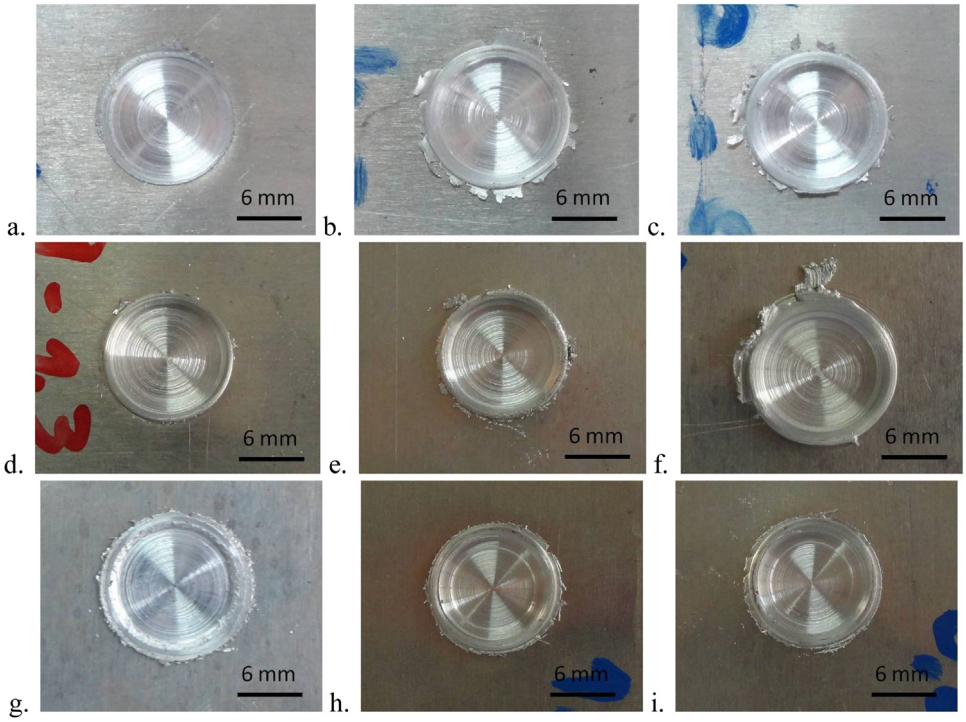

Fig. 6. Welds surface appearance: (a) 5-A, (b) 25-A, (c) 55-A, (d) 5-B, (e) 35-B, (f) 55-B, (g) 5-C, (h) 40-C and (i) 65-C.

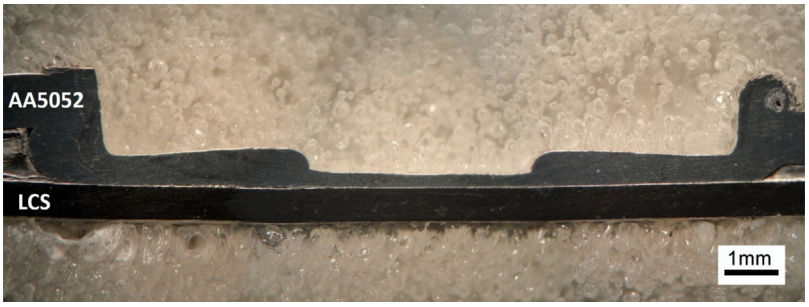

Fig. 7. Macrographic appearance of the weld 55-A.

It has been previously said that the TPD is the distance that the shoulder of the welding tools plunge into the aluminum sheet. According to [2], the largest part of the heat input in FSSW (of aluminum alloys) is due to the shoulders action. However, it is also important to know how close the whole tool gets to the interface. Therefore, not only the TPD values are important but also the P values. It is worth noticing that for the same level of TPD, the "C" tool presents the minimum P value as it may be seen in Table 3. Finally, despite it is possible to achieve low levels of P values with the three tools, the "A" and "B" tools would not present high mechanical properties. The "A" tool has a small pin and the "B" tool showed highly deformed spots for the minimum P values. So, taking into account the geometry of the "C" tool, it would optimize the mechanical properties in PT and CT.

3.2. Data acquisition

Fig. 9a and b shows the current consumed by the welding machine and the axial load during the welding process for samples 10-C and 50-C.

It can be seen that both measured values have a similar behavior. Initially, axial load and current increased throughout the tool penetration. During the dwell time, the plastized aluminum presents lower strength because of its heating, so the welding current and the axial load decrease. Finally, when the welding tool is retracted from the joint, the axial load and the current return to its initial values. It may be also seen in Fig. 9a that the maximum axial load is 6 kN, meanwhile the maximum current consumed by the machine is 17 A. However, it can be appreciated in Fig. 9b that the maximum

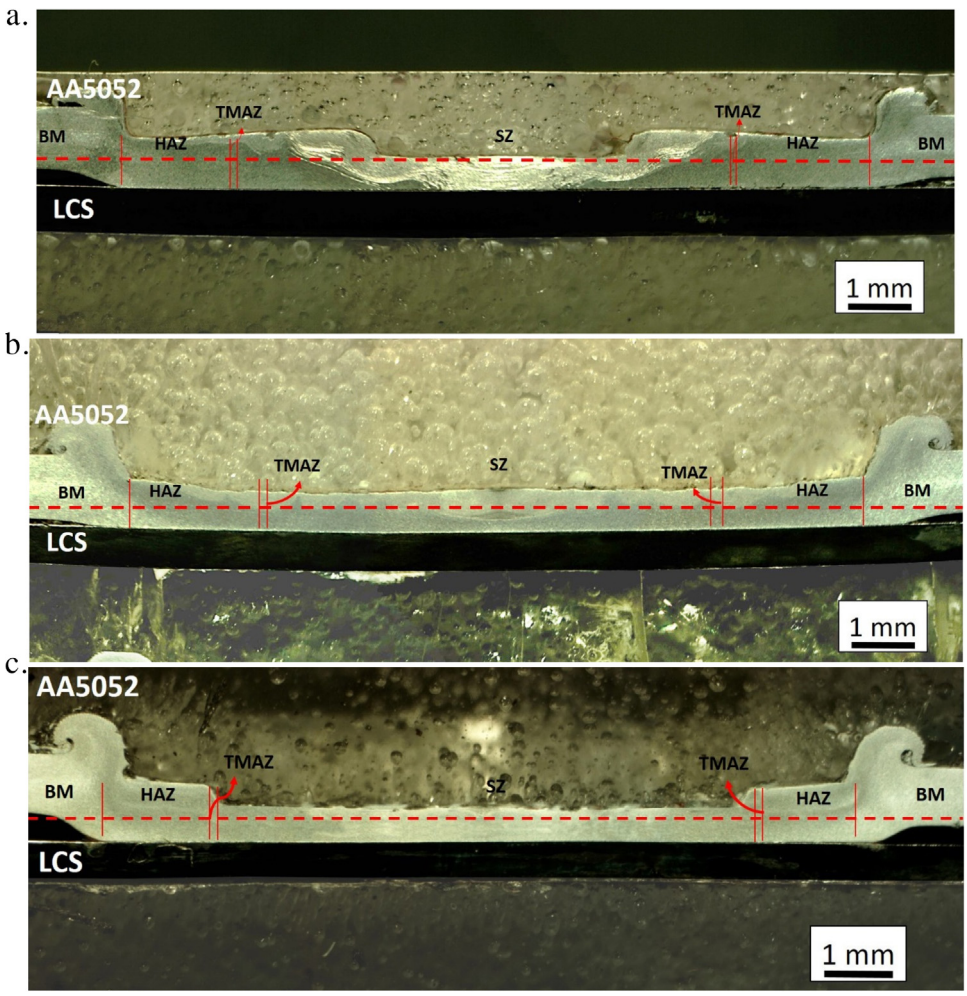

Fig. 8. Macrographic appearance of the welded joints: (a) 25-A, (b) 25-B and (c) 25-C.

Table 3
Main spots dimensions.

Sample	TPD (mm)	P (mm)	Welding Tool	IH (mm)	Fracture Mode
5-A	0.05	1.3	A	0.95	I
20-A	0.20	1.15	A	0.80	I
25-A	0.25	1.1	A	0.74	I
55-A	0.55	0.8	A	0.45	M
5-B	0.05	1.6	B	0.95	I
20-B	0.20	1.45	B	0.80	I
25-B	0.25	1.4	B	0.76	I
35-B	0.35	1.3	B	0.65	M
45-B	0.45	1.2	B	0.55	C
55-B	0.55	1.1	B	0.45	C
5-C	0.05	1.2	C	0.95	I
10-C	0.1	1.15	C	0.9	I
20-C	0.2	1.05	C	0.8	I-M
30-C	0.3	0.95	C	0.7	M
40-C	0.4	0.85	C	0.6	M-C
50-C	0.5	0.75	C	0.5	C
65-C	0.65	0.6	C	0.35	C

axial load is 11 kN and the maximum consumed current is 19 A. The peak values achieved for both current and axial load increased with TPD.

Fig. 9b shows a singularity in both signals at the same time position, next to their maximum. This could be related with the plastic instability that occurs on the top sheet when welding with high levels of TPD (Fig. 7). This was systematically observed for those samples that show the plastic collapse of the remnant ligament next to the shoulder end. This effect detected could be an interesting way to the on line evaluation of the quality of the welded spots and to detect the TPD limit, before plastic collapse occurrence.

The evolution of current and axial load maximum with the tool penetration depth, when welding with the "C" tool, may be seen in Fig. 10.

Both the current and the axial load increase with the TPD until it is 0.25 mm due to the higher volume of material to be deformed by the welding tool. From that indentation, the maximums present high standard deviation. This effect could be related with the plastic instability of the remaining aluminum under the tool, which occurs for high levels of TPD (Fig. 7). The TPD limit for this tool is 0.25 mm.

3.3. Interface analysis

The microstructure of the interface between the two sheets was analyzed. For the three welding tools used, the interfaces (at the center of the welded spots) for the same TPD, are continuous and defects free, as it is shown in Fig. 11a through c.

It can be seen in Fig. 11a to c how the aluminum sheet is forged against the steel sheet, developing the welding joint. According to the analysis made in the present work there is no evidence of plastic deformation in the steel sheet. It has been previously reported that local plastic deformation occurs in the steel sheet [16]. However, the results shown in [16] were achieved for high dwell times. In the present work, a short dwell time of only 2 s was used. This weld-

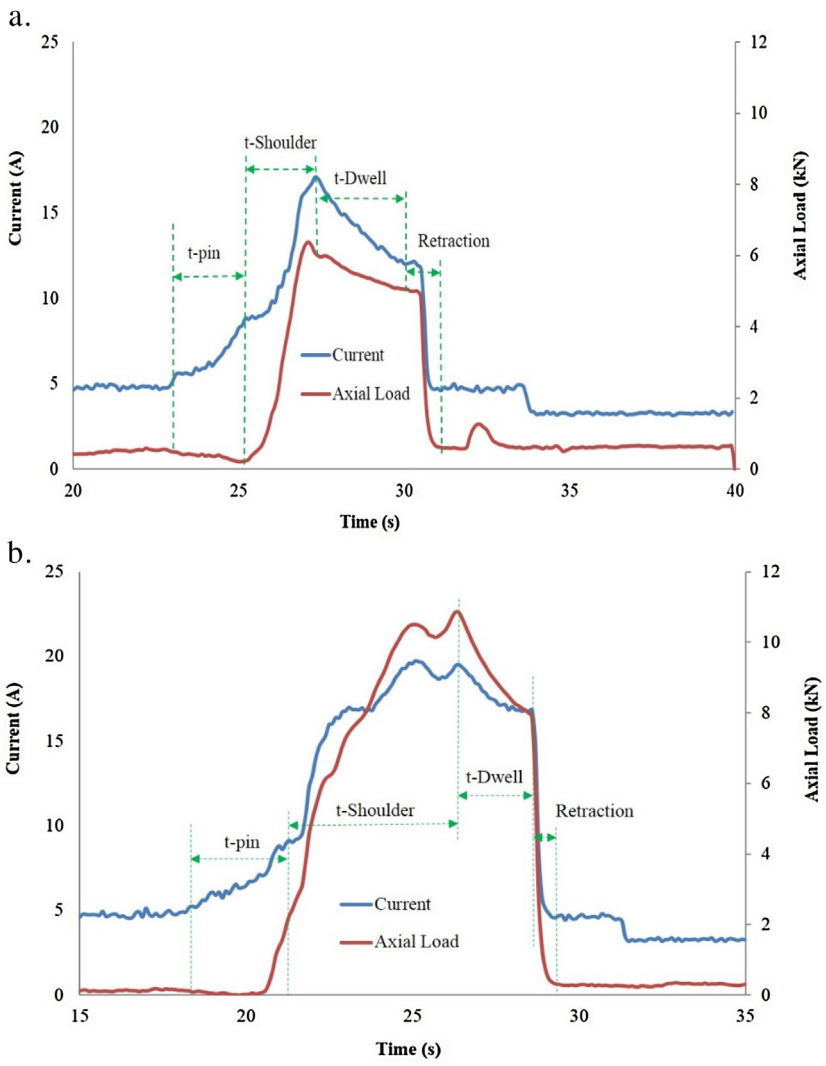

Fig. 9. Current and axial load signals during the welding cycle: (a) 10-C and (b) 50-C.

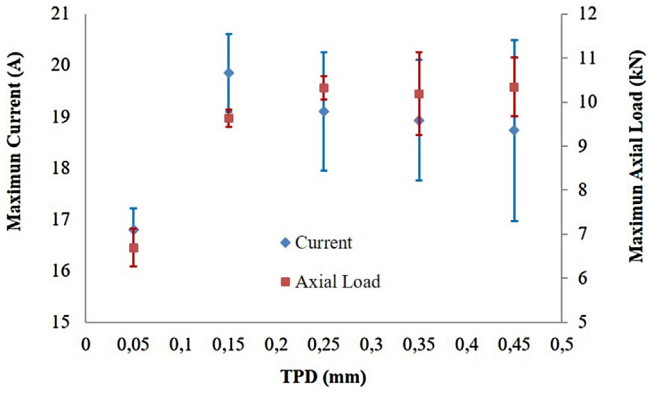

Fig. 10. Maximum current and axial load with the TPD for tool C.

ing parameter may be the main reason of no evidence of plastic deformation in the steel sheet.

It has been previously reported that when aluminum to galvanized steel joints are produced by FSSW, under the tool profile (in the aluminum sheet), it could be appreciated a dark zone. This dark zone could reach the surface of the top sheet according to the welding parameters used [10,12,17]. Different tests have been done in order to identify this dark zone and it was concluded that it is a fine dispersion of Zn particles into the aluminum matrix. This Zn particles dispersion is promoted by the tool action onto the joint interface [9]. In the present work a non-galvanized steel sheet is joined to an aluminum plate. In the interface of the welded joints it may be seen a thin layer of another phase (Fig. 11a–c). It has been demonstrated that this thin layer is an IMC formed during the thermal cycle produced by the action of the welding tool [10,16].

It is worth noting that there are differences in the interfaces when welding with different welding tools, for the same TPD. A relative non-continuous and thin layer of about 2.5 μm has been seen when welding with the "A" tool (Fig. 11a). On the other hand, when welding with the tool "B", a thicker and continuous layer of 3 μm has been observed at the interface, as it can be seen in Fig. 11b. Finally, a continuous and thicker layer (5 μm) was obtained when welding with the "C" tool (Fig. 11c). This behavior could be related to the effect of the tools geometry on the formation of the welded joints.

3.4. Vickers microhardness

In Fig. 12, the evolution of Vickers microhardness in the aluminum Plate 200 μm above the interface may be appreciated.

There had been no significant differences in the microhardness profiles while modifying the welding parameters. Hardness decreases from the Base Material (BM) (80 HV) through the Thermo

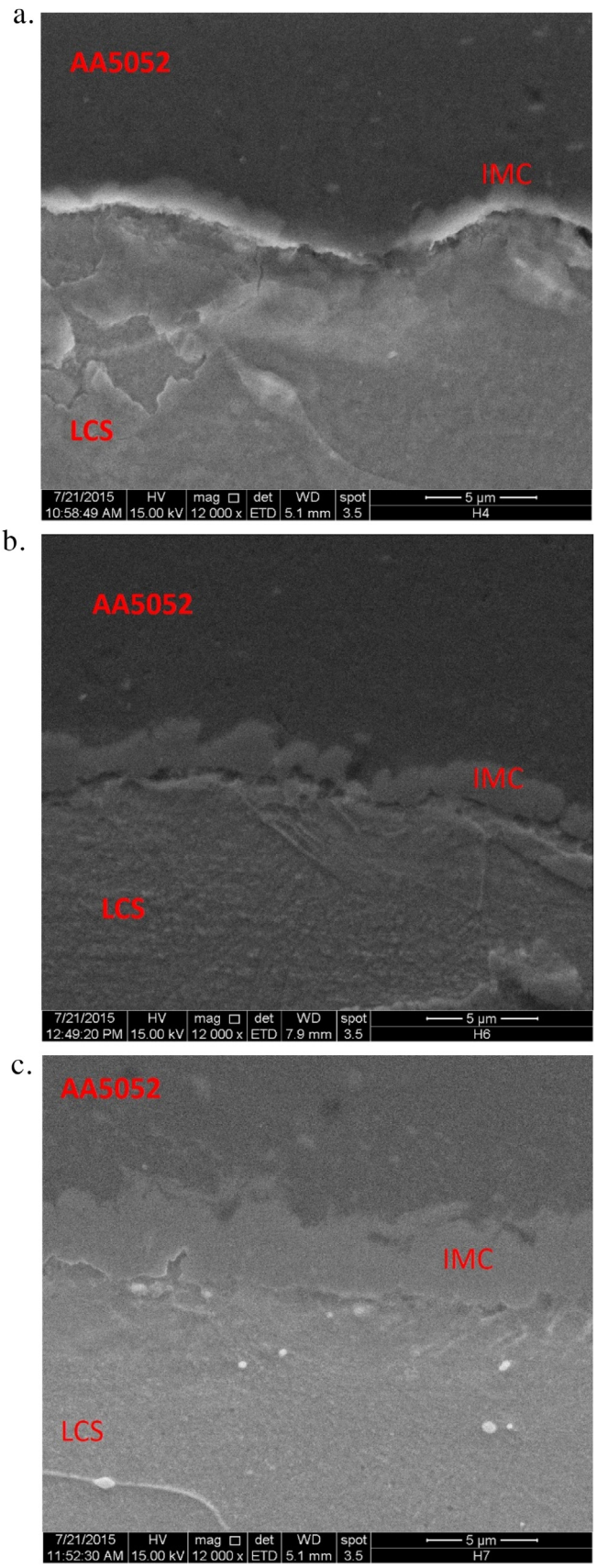

Fig. 11. SEM images of the welded interfaces: (a) 25-A, (b) 25-B and (c) 25-C.

Mechanical Affected Zone (TMAZ) and the Heat Affected Zone (HAZ), where the minimum is reached (55–65 HV).

In the HAZ the material has experienced a thermal cycle that has modified the microstructure and/or the mechanical properties because of the thermal cycle. However, there is no plastic deformation. The AA5052 used in the present paper was initially in a strain-hardened condition (H32). As a consequence of the experimented thermal cycle the top sheet suffers microstructural changes. In zones next to the nugget, the microstructure is fully recrystallized. The fraction of recrystallized material diminishes up to zero as the distance from the weld centerline increases, reaching the base metal condition [2].

The observed decreasing in hardness (Fig. 12) may be related to recrystallization inside the HAZ due to the welding thermal cycle, according to [2,18]. In non-heat treatable aluminum alloys, with some amount of previous cold work, there is a continuous declining area fraction of recrystallized material. The recrystallized material that is outside of the Stir Zone (SZ) is material that is produced by the thermal cycle associated with the welding process. Recrystallization in this region is driven by the cold work that is already present in the base material and not by deformation associated with the FSSW process [2]. The obtained results agree with what it has been previously reported elsewhere for similar joints [19]. Finally, it should be noted in Fig. 12 that inside the SZ, hardness is higher than in the HAZ but lower than in the BM. It has been demonstrated that inside the SZ there is dynamic recrystallization because of plastic deformation and increased temperature, which produces a fine grain structure, rising hardness values [2].

In the same sense, there is no big difference in the microhardness profiles when welding with “A”, “B” or “C” tool. Nevertheless all the microhardness profile is located at a low hardness value for tool “C”. This could be related to the higher heat input at the interface by this tool, due to its design, producing higher softening in the material adjacent to the interface.

3.5. Peel and cross tension tests

The evolution of the fracture load in PT with the TPD may be seen in Fig. 13, for the three welding tools analyzed. It is shown that the fracture load rises up to reach a maximum and then decreases with the TPD, for the three welding tools.

It may be appreciated in Fig. 13 that for the same TPD, the fracture loads of the joints welded with the “C” tool are higher than the ones achieved with the “B” and “A” tools.

The results of CT tests are shown in Fig. 14. The obtained values were not significant affected by TPD, but it can be seen a tendency to increase the fracture load with TDP. The best results were obtained again for tool “C”. According to the achieved fracture loads in CT tests, more work has to be done in order to improve mechanical properties with the welding parameters.

The fracture surfaces of PT of three samples welded with “A”, “B” and “C” tools may be seen in Fig. 15a–c. It can be appreciated that not only the fracture loads, but also the fracture modes are modified by the welding geometry and TPD.

4. Discussion

4.1. Formation of the IMC

Metallurgical bonding between both aluminum and steel sheets is a result of atomic diffusion in the interface [12,13,16,20–22]. It has been previously reported that Al/Fe IMC would grow in the interface because of atomic diffusion, if enough energy is supply by the welding tool to the joint interface [12,13,16,20,21,23]. The composition, morphology and also the thickness of the inter-

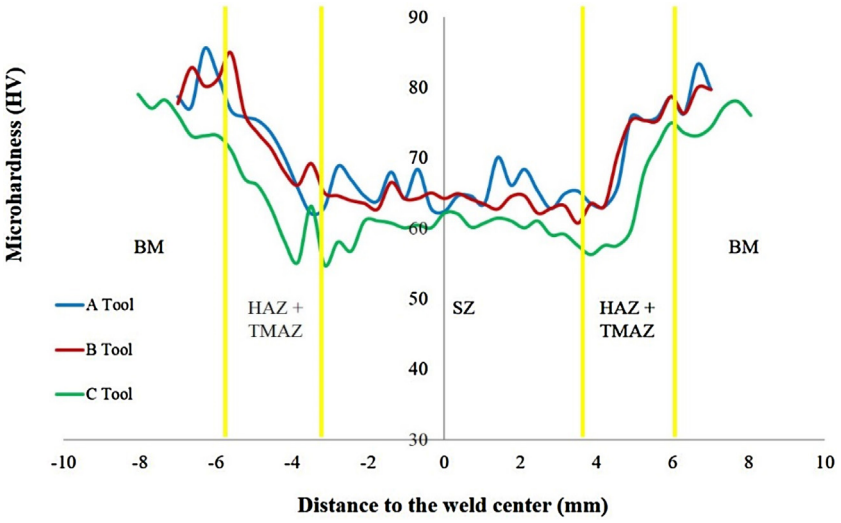

Fig. 12. Vickers microhardness profiles.

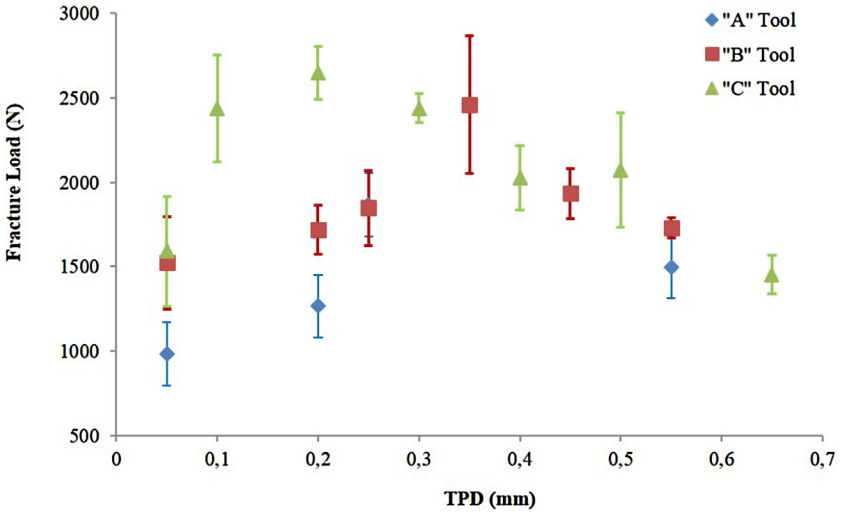

Fig. 13. Fracture load vs TPD in Peel Tests.

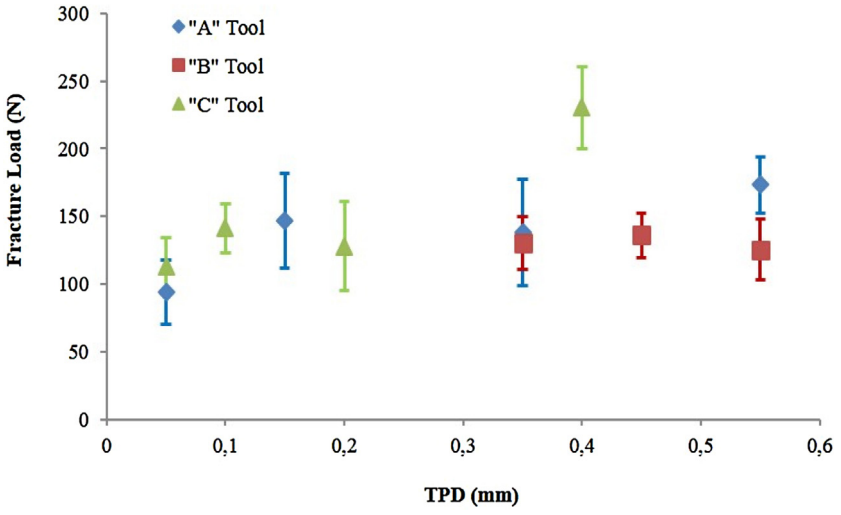

Fig. 14. Fracture load vs TPD in Cross Tension Tests.

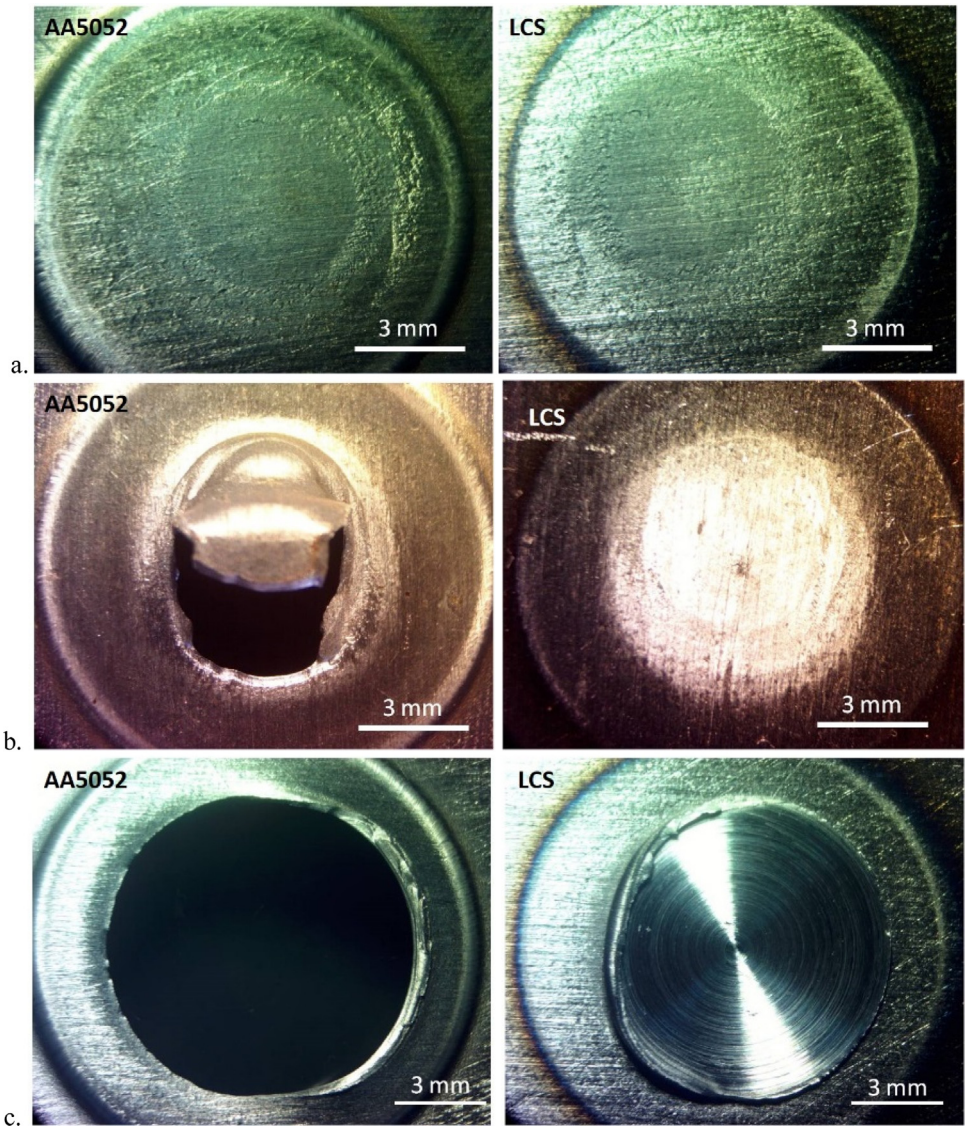

Fig. 15. Fracture surfaces of PT: (a) 20-B, (b) 55-A and (c) 65-C.

metallic layer are mainly established by nucleation and growth. They depend on stored energy, in terms of temperature and plastic deformation at the interface. According to [21] Zn-coatings on steel can be regarded as beneficial in solid–solid joining procedures, improving bonding by rapid dissolution. So, a controlled formation of even and regular reaction layers may be achieved. There are several studies where the formation mechanism and shape of the IMC are reported [24]. According to [25], the interfacial reaction layer decreases the weld strength due to the crack formation. In the same sense, the thickness and shape of the intermetallic layer plays a critical role on the mechanical properties of the welds [25]. However, according to [11,12], an IMC layer seems to be necessary to improve the weld strength, but if the IMC layer is too thick cracks initiate and propagate easily through it. Finally, the type of IMC that is formed in the interface depends on the cycle time that the interface experiments [23].

In FSSW, the increased temperature produced by the action of the welding tool, is the activation energy for the nucleation and growth of IMC at the interface between both sheets. Finally, high pressure in the joint interface due to the axial load of the welding tool, improves atomic diffusion in that zone [20].

Reducing the pin length allows the tools shoulder to go deeper into the aluminum sheet. This effect produces higher temperatures at the interface and higher material flow next to it, due to greater thermomechanical action of the tool shoulder on the interface [2,8,15]. Moreover, as much as the shoulder gets close to the interface, the axial load is increased (as it may be seen in Fig. 9), improving the diffusion effect in the interface of both sheets.

As it may be seen in Fig. 11a through c, there are several differences in the morphology and thickness of the IMC formed in the welded joints. The evolution of the IMC from non-continuous to continuous and the increase of intermetallic layer thickness with the tools used, show the effect of their geometry on the thermomechanical effect at the interface. The results shown in Fig. 11 are of samples achieved with the same level of TPD, at the center of the welded joints.

The evolution of the IMC thickness along the interface of both sheets under the welding tools, for a TPD of 0.25 mm may be appreciated in Fig. 16. It can be seen that not only the thickness of the IMC (at the center of the welded joint) depends on the tools geometry, but also the nucleation and growth of IMC along the whole interface. For the “A” tool the IMC was only seen under the pin profile and not away from it. The maximum thickness was achieved at

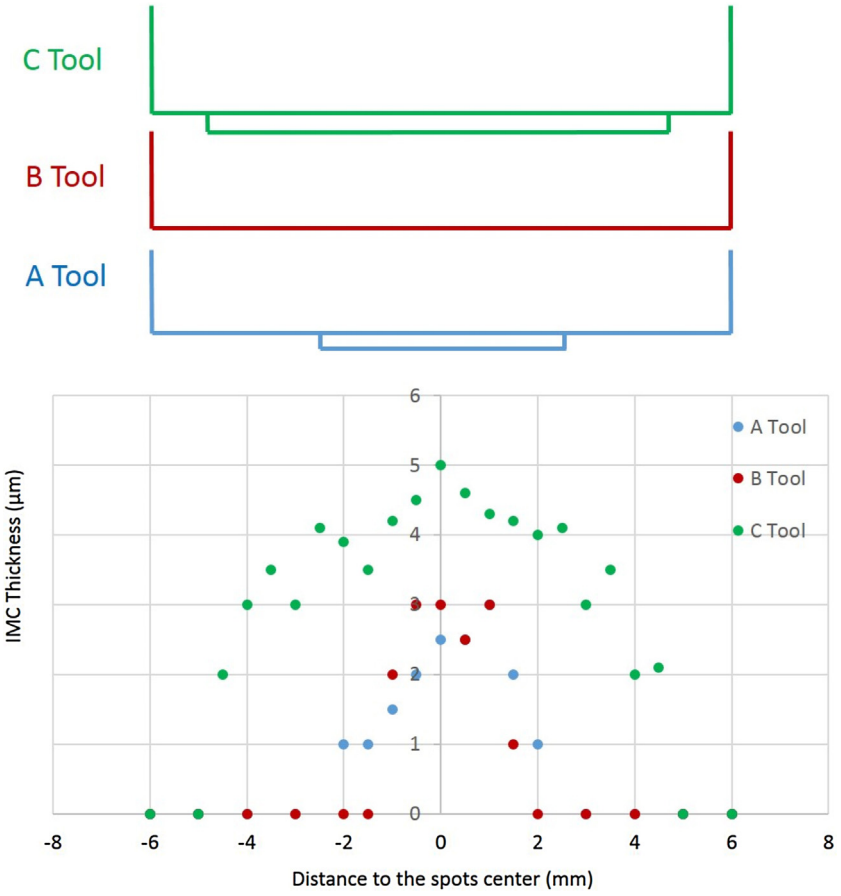

Fig. 16. Evolution of IMC thickness along the interface for TPD = 0.25 mm.

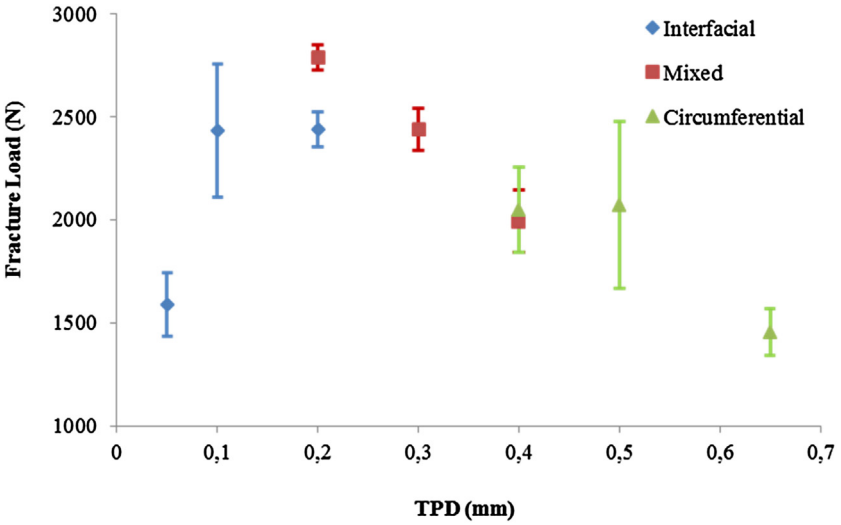

Fig. 17. Fracture mode evolution in Peel Tests for C tool.

the weld center. In the same sense, the nucleation and growth of the IMC for the "B" tool was viewed also in the center of the weld. Finally, when welding with the "C" tool, the IMC was also formed below the pin profile, but in this case the thickness of IMC is higher.

According to [26], in the central region of the tool, the material surface velocity increases proportionally with radius, representing sticking contact. However, it must reach a maximum value and fall to zero close to the tool edge, for continuity with the surrounding stationary material. This gives slip over some outer annular portion of the contact, with frictional heat generation restricted to this region, superimposed on volumetric plastic dissipation under the whole contact area. Furthermore, the thermal field shows the maximum temperatures at the center of the welds [26,27]. The IMC thickness distribution along the Al/St interface in [26] shows the same behavior that may be seen in Fig. 16.

On the other hand, the fact that the thickness of the IMC increases from the peripheries of the spots to their center could also be related to the pressure distribution under the pin. While the

sliding component of heat increases with the distance to the spot center due to the higher tangential velocity, near the periphery of the pin the pressure decreases due to the plastic flow of material. This higher pressure at the center of the spot controls the interdiffusion of Al and Fe, leading to the thicker IMC in this zone, as it was observed in Fig. 16.

So, not only the shape and thickness of the IMC depends on the tools geometry, but also its length. It is worth noting that more diffusion has been produced when welding with the "C" tool and larger bonded areas have been achieved.

4.2. Welding parameters/fracture load relationship

As it may be appreciated in Fig. 13 the mechanical properties of the welded spots are influenced by the effect of the TPD and the tools geometry. The joints welded with the "A" tool showed the lowest fracture loads for all the TPD. These results are related to the tools geometry. When joints were welded with the "A" tool, it has been appreciated that the aluminum sheet is highly deformed in the spot area. The maximum plastic deformation of the top sheet was achieved when welding with the "A" tool. This effect reduces the effective pressure on the interface (thus diffusion is decreased) because of top sheet plastic instability. Taking into account these results, the effective pressure during the FSSW process would be the lowest when welding with the "A" tool. The results achieved in peel tests agree with the IMC behavior, as it was previously discussed. Therefore, the thermomechanical input to the joints interface is the minimum. On the other hand, when the "B" tool is used, it is possible to get close to the interface with less plastic deformation of the top sheet, so the thermomechanical effect of the tool in that zone is higher. Therefore, the fracture loads are higher than the ones obtained with "A" tool. Finally, the proposed design for the "C" tool allows the pin and shoulder of the tool to maximize the energy input to the interface (larger bonded areas as seen in Fig. 16), without excessive deformation of the top sheet, achieving the highest fracture loads.

It has been previously reported that a "pull-out" fracture mode is related to properly welded joints (defects free) and will present high shear strength. This fracture mode may also present certain levels of plastic deformation during the test. On the other hand, an interfacial fracture mode implies low fracture loads and no plastic deformation during the test, failing in a brittle manner [28].

As it may be appreciated in Fig. 15a, when welding with low levels of TPD the fracture mode is interfacial. The samples that presented this type of fracture mode did not reach high fracture loads. On the contrary, it may be seen in Fig. 15b that a mixed fracture mode occurs for optimum values of indentation, taking into account that samples which presented this fracture mode reached the maximum fracture loads. Finally, the third fracture mode was circumferential, as it is shown in Fig. 15c. Samples that showed this type of fracture mode, presented lower fracture loads than the ones that failed with a mixed mode. This effect is related to the great reduction of the remaining aluminum (IH). Despite the fracture load is not the highest, the samples that failed with a circumferential mode showed plastic deformation due to fracture along the aluminum sheet. The fracture mode of each sample could be seen in Table 3, where "I" is Interfacial, "M" is Mixed and "C" is Circumferential fracture mode.

While higher TPD imply the increase of heat input on the interface, improving the fracture load, excessive thinning of the top plate produces the decrease of fracture loads for the highest levels of indentations [15].

The evolution of fracture modes in PT with TPD for tool "C" is shown in Fig. 17. The highest fracture loads were achieved in the transition zone between the interfacial and mixed fracture modes. This effect could be related to the improvement of the interface strength with the increase of the TPD and excessive the reduction of IH.

Taking into account the increase of the intermetallic layer (thickness and length) with the tools geometry and the evolution of fracture load in PT, it could be thought that the increase of the intermetallic layer is an evidence of improving the diffusion effect, so spot welds of better quality are achieved.

Regardless the detrimental effect of the IMC in the interface of dissimilar joints shown by [6,10,11,24,29], it has been previously reported that an IMC layer seems to be necessary to improve the weld strength. However, if the IMC layer is too thick cracks initiate and propagate easily through the brittle IMC tangles [23,30,31]. An optimal IMC layer thickness of 8 μm was found to be optimal for improving mechanical properties in PT [23]. In the present work the best mechanical properties were achieved for the "C" tool where the thicker and larger IMC was found. So, the formation of and IMC up to five microns raises the mechanical properties.

It has been previously said that the fracture loads in CT tests were not significant affected by TPD, but it can be seen a tendency to increase the fracture load with TDP. Taking into account the mechanical properties shown in Figs. 13 and 14, the best results have been achieved with the "C" tool. The maximum fracture loads in PT and CT tests have not been achieved for the same TPD. Despite this effect, it could be concluded that the optimal range of TPD is between 0.2 and 0.4 mm, where the maximum fracture loads have been achieved as well as mixed and circumferential fracture modes.

Higher fracture loads than the ones previously reported in PT and CT tests [9,13,14,16], with lower dwell times, have been achieved in the present work. This aspect confirms the potential as a technological applicable process by improving the quality of dissimilar joints in thin sheets. In the same sense, productivity has been improved by welding with only 2 s of dwell time.

5. Conclusions

- Friction stir spot welds on dissimilar joints of AA5052-LCS, of 1 and 0.65 mm thick, have been made with tools made of conventional, low cost, H13 tool steel. Defects free and excellent appearance joints have been achieved.
- The maximum values of the consumed current and the axial load increase with the TPD, until the plastic instability of the top sheet (IH) occurs, for highest levels of TPD. For this TPD both signals show a drop, indicating the occurrence of the plastic instability. This can be used as an on-line monitoring technique.
- The tools geometry changes the thickness, shape and length of the intermetallic layer formed. The welds done with the "C" tool have the most continuous and thickest intermetallic layer of 5 μm. The maximum bonded areas have been achieved with the "C" tool. The intermetallic layer thickness increase could be related to the higher heat input by the optimization of the welding tool geometry.
- The "C" tool has optimized the fracture load of the welded joints with a dwell time of only 2 s. This aspect confirms its potential as a technological applicable process in terms of quality and productivity.
- For low levels of indentation, the fracture mode is interfacial. For higher TPDs, the fracture mode is mixed (maximum fracture load). The highest levels of TPD have produced a circumferential fracture mode with lower fracture loads but with higher levels of plastic deformation.
- The optimized geometry of the tool (pin diameter and length) with a correct TPD value can maximize the mechanical properties of the joint, through the heat reaching the interface, the bonded area under the pin and the pressure in this zone, diminishing the time required for a good joint.

Acknowledgements

The authors of the present paper would like to thank Agencia Nacional De Promoción Científica y Tecnológica and the Universidad de Buenos Aires for the financial support of this paper.

References

[1] Shome M, Tumuluru M. Welding and joining of advanced high strength steels (AHSS). Oxford: Elsevier; 2015.
[2] Mishra R, Mahoney M. Friction stir welding and processing. Ohio: ASM International; 2007.
[3] European Aluminium Association, The Aluminium Automotive Manual, http://c.ymcdn.com/sites/www.aec.org/resource/resmgr/PDFs/1-Intro_2015.pdf, 2015 (Accessed 26 June 2015).
[4] Kumar N, Yuan W, Mishra R. Friction stir welding of dissimilar alloys and materials. Oxford: Elsevier; 2015.
[5] Ambroziak A, Korzeniowski M. Using resistance spot welding for joining aluminium elements in automotive industry. Arch Civil Mech Eng 2010;10:1–13.
[6] Chen Y, Komazaki T, Kim Y, Tsumura T, Nakata K. Interface microstructure study of friction stir lap joint of AC4C cast aluminum alloy and zinc-coated steel. Mater Chem Phys 2008;111:375–80.
[7] Francesco L, Svoboda H. Efecto de las variables de proceso de Soldadura de Punto por Fricción Agitación (FSSW) de aluminio en las propiedades mecánicas. Buenos Aires: FIUBA; 2013.
[8] Tozaki Y, Uematsu Y, Tokaji K. Effect of tool geometry on microstructure and static strength in friction stir spot welded aluminium alloys. Int J of Mach Tools Manuf 2007;47:2230–6.
[9] Miyagawa K, Tsubaki M, Yasui T, Fukumoto M. Spot welding between aluminum alloy and Zn coated steel by friction stirring. Q J Jap Wel Soc 2008;26:131–6.
[10] Elrefaey A, Takahashi M, Ikeuchi K. Friction-stir-welded lap joint of aluminum to zinc-coated steel. Q J Jap Wel Soc 2005;23:186–93.
[11] Shen Z, Chen Y, Haghshenas M, Gerlich A. Role of welding parameters on interfacial bonding in dissimilar steel/aluminum friction stir welds. Eng Sci Tech 2015;18:270–7.
[12] Haghshenas M, Abdel-Gwad A, Omran A, Gökçe B, Sahraeinejad S, Gerlich A. Friction stir weld assisted diffusion bonding of 5754 aluminum alloy to coated high strength steels. Mater Des 2014;55:442–9.
[13] Tanaka K, Kumagai M, Yoshida H. Dissimilar joining of aluminum alloy and steel sheets by friction stir spot welding. J Jap Inst L Metals 2006;56:317–22.
[14] Tran V, Pan J. Fatigue behavior of dissimilar spot friction welds in lap-shear and cross-tension specimens of aluminum and steel sheets. Int J Fatigue 2010;32:1167–79.
[15] Piccini J, Svoboda H. Effect of the tool penetration depth in friction stir spot welding (FSSW) of dissimilar aluminum alloys. Proc Mater Sci 2015;8:868–77.
[16] Fereiduni E, Mavahedi M, Kokabi A. Aluminum/steel joints made by an alternative friction stir spot welding process. J Mater Process Tech 2015;224, 1–0.
[17] Piccini J, Svoboda H. Effect of pin length on friction stir spot welding (FSSW) of dissimilar aluminum-steel joints. Proc Mater Sci 2015;9:504–13.
[18] Dieter G. Mechanical metallurgy. Liverpool: McGraw-Hill; 1988.
[19] Shen Z, Yang X, Yang S, Zhang Z, Yin Y. Microstructure and mechanical properties of friction spot welded 6061-T4 aluminum alloy. Mater Des 2014;54:766–78.
[20] Mehrer H. Diffusion in Solids, Fundamentals, Methods, Materials, Diffusion-Controlled Processes. Berlin: Springer-Verlag; 2007.
[21] Springer H, Szczepaniak A, Raabe D. On the role of zinc on the formation and growth of intermetallic phases during interdiffusion between steel and aluminium alloys. Acta Mater 2015;96:203–11.
[22] Taban E, Gould J, Lippold J. Dissimilar friction welding of 6061-T6 aluminum and AISI 1018 steel: properties and microstructural characterization. Mater Des 2010;31:2305–11.
[23] Bozzi S, Helbert-etter A, Baudin T, Criqui B, Kerbiguet J. Intermetallic compounds in Al 6016/IF-steel friction stir spot welds. Mater Sci Eng 2010;527:4505–9.
[24] Sun Y, Fujii H, Takaki N, Okitsu Y. Microstructure and mechanical properties of dissimilar Al/steel joints prepared by a flat spot friction stir welding technique. Mater Des 2013;47:350–7.
[25] Springer H, Kostka A, Payton E, Raabe D, Kaysser-Pyzalla A, Eggeler G. On the formation and growth of intermetallic phases during inter diffusion between low-carbon steel and aluminum alloys. Act Mater 2011;59:1586–600.
[26] Jedrasiak P, Shercliff H, Reilly A, McShane G, Chen Y, Wang L, et al. Thermal modeling of al-Al and Al-steel friction stir spot welding. J Mater Eng Perform 2016;25(9):4089–98.
[27] Awang M. Simulation of Friction Stir Spot Welding (FSSW) Process: Study of Friction Phenomena. PhD thesis. University of West Virginia; 2007.
[28] Tran V, Pan J, Pan T. Effects of processing time on strengths and failure modes of dissimilar spot friction welds between aluminum 5754-O and 7075-T6 sheets. J Mater Process Technol 2009;209:3724–39.
[29] Coelho R, Kostka A, DosSantos J, Kaysser-PyzallaTaban A. Friction-stir dissimilar welding of aluminium alloy to high strength steels: mechanical properties and their relation to microstructure. Mater Sci Eng A 2012;556:175–83.
[30] Liedl G, Bielak R, Ivanova J, Enzinger N, Figner G, Bruckner J, et al. Joining of aluminum and steel in car body manufacturing. Phys Proc 2011;12:150–6.
[31] Liu X, Lan S, Ni J. Analysis of process parameters effects on friction stir welding of dissimilar aluminum alloy to advanced high strength steel. Mater Des 2014;59:50–62.